FEBS Letters 585 (2011) 1864–1872

journal homepage: www.FEBSLetters.org

Homeoprotein Hbx4 represses the expression of the adhesion molecule DdCAD-1 governing cytokinesis and development

Ji-Sun Kim, Ji-Hui Seo, Hyung-Soon Yim, Sa-Ouk Kang *

Laboratory of Biophysics, School of Biological Sciences, and Institute of Microbiology, Seoul National University, Seoul 151-742, Republic of Korea

ARTICLE INFO

Article history:
Received 31 March 2011
Accepted 11 April 2011
Available online 28 April 2011

Edited by Dietmar J. Manstein

Keywords:
Homeobox
Adhesion molecule
Cytokinesis
Development

ABSTRACT

We investigated the function of homeodomain-containing protein Hbx4 in *Dictyostelium discoideum*. Hbx4-overexpressing cells (Hbx4^{OE}) displayed defects in growth rate and cytokinesis and showed differences in slug motility and cell-type proportioning from KAx3. Furthermore, the overexpression of Hbx4 inhibited the induction of *cadA*, which encoded the Ca^{2+}-dependent cell adhesion molecule DdCAD-1, despite expression of *csaA* and *gpaB*. The electrophoretic mobility shift assay showed that the promoter of *cadA* contained the Hbx4-binding site. Moreover, constitutively expressed DdCAD-1 in Hbx4^{OE} rescued the defects in cytokinesis and development. These results suggest that Hbx4 modulates DdCAD-1-mediated cytokinesis and cell-type proportioning.

1. Introduction

Homeobox (Hox) genes encode proteins with a highly conserved helix-turn-helix DNA-binding homeodomain and function as transcription factors by directly binding to DNA sequences in Hox response elements. After being identified from a homeotic mutation in a body segmentation disorder in *Drosophila*, Hox genes have been recognized as important regulators in body segment during differentiation and development. Recent studies show that Hox genes modulate proliferation and the cell cycle [1–3]. Furthermore, Hox genes have been involved in both the proliferation of hematopoietic cells and translocation events in leukemic cells, implying that they may be important in oncogenesis [4].

In *Dictyostelium discoideum*, there are 14 predicted Hox genes with one duplicate on chromosome 2. The genes *hbx1* (*wariai*) and *hbx2* control cell-type differentiation and cell-type proportioning, and *hbx*3 plays a role during phagocytosis [5,6]. To evaluate the role of Hox in *D. discoideum*, we cloned *hbx4*, which possessed a highly conserved homeodomain (Fig. 1A). Cells that constitutively expressed Hbx4 exhibited defects in cytokinesis and development. We also observed that DdCAD-1 was markedly repressed in Hbx4-overexpressing cells (Hbx4^{OE}). Furthermore, the overexpression of DdCAD-1 in Hbx4^{OE} rescues the defects in cytokinesis and development. These findings suggest that, in addition to cell–cell adhesion [7], DdCAD-1 may function in cytokinesis during growth. In the current study, we show that Hbx4 regulates cytokinesis and cell-type proportioning by modulating DdCAD-1.

2. Materials and methods

2.1. Cell culture and development

KAx3 and the derived transformants were grown in HL5 medium and transferred to a non-nutrient agar plate as previously described [8]. Cells were also grown in shaking suspension using the following method: washed cells were developed in KK2 suspension at a density of 1×10^7 cells/ml and shaken at 150 rpm and 22 °C. After 2 h, cAMP stimulation was performed by the addition of 30 nM cAMP every 6 min [9].

2.2. Cloning of hbx4 gene and strain construction

To overexpress Hbx4 in *D. discoideum*, the full-length gDNA of *hbx4* was ligated into the pTX-FLAG vector. To generate a knockout strain, the full-length gDNA of *hbx4* was digested at the *Eco*RI site in *hbx4* and ligated to a 1.3 kb *Bam*HI fragment containing a blasticidin S resistant cassette from the SL63 vector. Constructs that overexpress or disrupt Hbx4 were introduced into KAx3 using electroporation. G418 (10 μg/ml) was used for selection of Hbx4^{OE}, and blasticidin S (10 μg/ml, Sigma) was used for *hbx4*$^-$. To overexpress DdCAD-1 in KAx3 and Hbx4^{OE}, the NotI fragment that contained

Abbreviations: DAPI, 4′,6-diamidino-2-phenylindole; TRITC, tetramethylrhodamine-5-(and 6-isothiocyanate; rpm, revolutions per minute; PST-A, prestalk-A region; PST-AB, prestalk-AB region; PST-O, prestalk-O region; ALCs, anterior-like cells; EMSA, electrophoretic mobility shift assay; IPTG, isopropyl-β-D-thiogalactopyranoside; DIF, differentiation-inducing factor

* Corresponding author. Fax: +82 2 888 4911.
E-mail address: kangsaou@snu.ac.kr (S.-O. Kang).

0014-5793/$36.00
doi:10.1016/j.febslet.2011.04.052

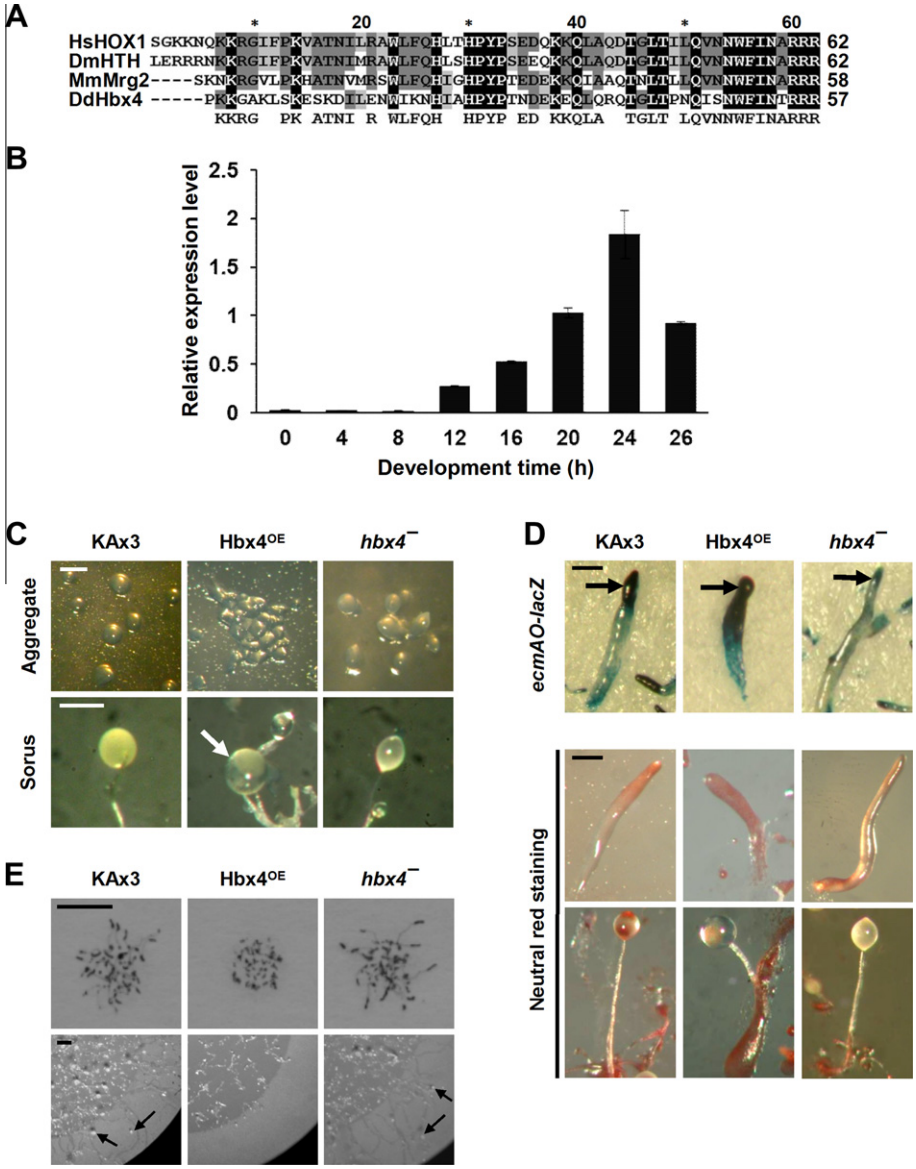

Fig. 1. Hbx4^{OE} exhibits defects in developmental morphology. (A) The multiple alignment of the deduced amino acid sequences of *D. discoideum* Hbx4 (DdHbx4) with those of *Homo sapiens* homeoprotein (HsHOX1), *Drosophila melanogaster* Homothorax (DmHTH), and *Mus musculus* Mrg2 protein (MmMrg2) is shown. Identical residues are indicated with shaded letters. (B) The determination of the expression level of *hbx4* by real-time RT-PCR is shown. The values represent the mean ± S.E.M. of three independent experiments. (C) The phenotypes of KAx3 and Hbx4 mutant strains developed on KK2 agar plates are shown. Scale bar: 0.5 mm. (D) The analysis of aberrant cell-type proportioning is shown. The upper panels show spatial patterning of each strain by β-gal histochemical analysis. *ecmAO* is expressed in the anterior prestalk domain (arrowhead points). The lower panels are slug (upper images) and fruiting body (lower images) that were stained with neutral red dye. Scale bar: 0.4 mm. (E) The analysis of the slug migration is shown. The upper panels show slug trails. Scale bar: 10 mm. The lower panels show the location of the fruiting body produced after migration. Arrows indicate the fruiting bodies that formed outside the plot zone. Scale bar: 5 mm.

the G418 resistant cassette in Exp4(+) vector was substituted with the *Bam*HI fragment that contained a blasticidin S resistant cassette from SL63. DdCAD-1 cloned to Exp4(+) vector that contained blasticidin S resistant cassette. This construct was transfected into KAx3 and Hbx4^{OE}. CAD1^{OE}/Hbx4^{OE} was selected in HL5 medium containing blasticidin S and G418.

2.3. Real-time RT-PCR

Each RNA sample (50 ng/μl) was reverse transcribed into cDNA using a superscript III reverse transcriptase kit (Promega). Each PCR was performed with SYBR Premix Ex Taq (TaKaRa) and *rnlA* was used as the endogenous control gene. Cycle threshold values of each gene were normalized to *rnlA* and calibrated to an average expression level for the gene being analyzed.

2.4. Neutral red and histochemical staining

The cells cultured in HL5 were stained in 0.03% neutral red (Sigma) and developed in the dark at 22 °C [10]. Neutral red is used to stain the acidic vacuole found in prestalk cells and ALCs, to quantify sizes of prestalk compartments, and to monitor movement of ALCs within the prespore region. To observe the spatial expression of the prestalk cells, cells were transformed with *ecmAO/lacZ* constructs in which β-gal is expressed from *ecmAO*-specific promoter. *ecmAO* is expressed in prestalk cells that are localized in the anterior

Table 1
Primer sequences for *cadA* promoter.

Probe	Primer	Sequence
A	Forward	GTTGTATTAAATTTAAAAAAAGAAGATTGG
	Reverse	GATTTATTAAGTTGAAACAAGTTGC
B	Forward	GTTGTATTAAATTTAAAAAAAGAAGATTGG
	Reverse	CCATTTACAATTATTTTTTATTTC
C	Forward	CCTGATGGTGATGATGGTTATGATG
	Reverse	GAGAAGTTTTTTAATTTTTTACCAC
D	Forward	GCAACTTGTTTCAACTTAATAAATC
	Reverse	GAGAAGTTTTTTAATTTTTTACCAC
E	Forward	CCACACCAATGATTTAAATCTCAC
	Reverse	GACATTTTTTAATTTTTAATACTATACC
F	Forward	CGGTTTTTTTGGATTATTTTCACAC
	Reverse	GACATTTTTTAATTTTTAATACTATACC
G	Forward	TAATTAGTATTATTCCTGATGGTG
	Reverse	TAATTGATTTATTAAGTTGAAAC
H	Forward	CCTGATGGTGATGATGGTTATG
	Reverse	GATTTATTAAGTTGAAACAAGTTGC
I	Forward	CCTGATGGTGATGATGGTTATG
	Reverse	AGATTTTAAAATTATTAATAATTCTG

region of slug. *ecmAO/lacZ*-marked cells were developed, fixed and stained for β-galactosidase activity as described previously [11].

2.5. Spore viability assay

To determine the number of viable spores [12], cells of 2×10^6 cells/cm^2 were developed on the KK2 agar plate. After 2 days, their spores were incubated in KK2 buffer containing 0.3% Triton X-100 for 10 min and washed three times with KK2. Spores were stained in 0.05% Calcofluor white ST for 10–20 min and visualized using the DAPI-channel filter of Axiolab microscope (Carl Zeiss). For the spore viability assay, spores were serially diluted and plated with *K. pneumoniae* on SM agar plates.

2.6. Fluorescence microscopy

Log-phase cells grown in suspension were observed as described previously [13]. To stain F-actin, cells were incubated

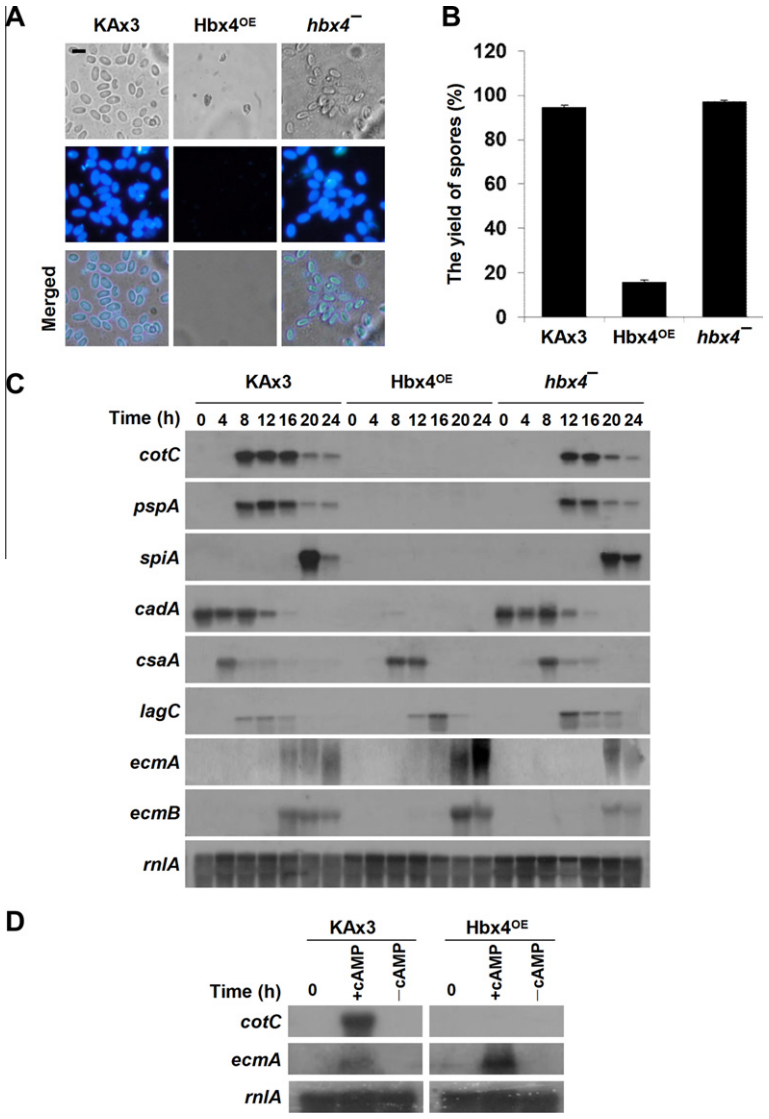

Fig. 2. Hbx4^{OE} exhibits defect in the production of viable spores. (A) Spore viability assay is shown. The upper panels are phase-contrast images of spores before treatment with Triton X-100. The middle panels are spores, which were treated with Triton X-100 and stained with the Calcofluor dye. Merged images are shown in the lower panels. Scale bar: 6 μm. (B) Spore yield was determined. The values represent the mean ± S.E.M. of three independent experiments. (C) The expression analysis of genes related to development. Northern blots were performed using fragments of the indicated genes as hybridization probes. *cotC* and *pspA*, prespore-specific; *spiA*, spore-specific; *cadA* and *csaA*, aggregation-specific; *lagC*, post-aggregative genes; *ecmA* and *ecmB*, prestalk-specific; *rnlA* was used as a loading control. (D) The induction of prestalk and prespore gene expression in suspension development. Cells were pulsed every 6 min with 30 nM cAMP for 4 h to maximize expression of cAMP receptors and aggregation-stage genes. Samples were incubated without cAMP or with 300 mM cAMP (supplemented every 2 h with 150 mM cAMP) for 6 h.

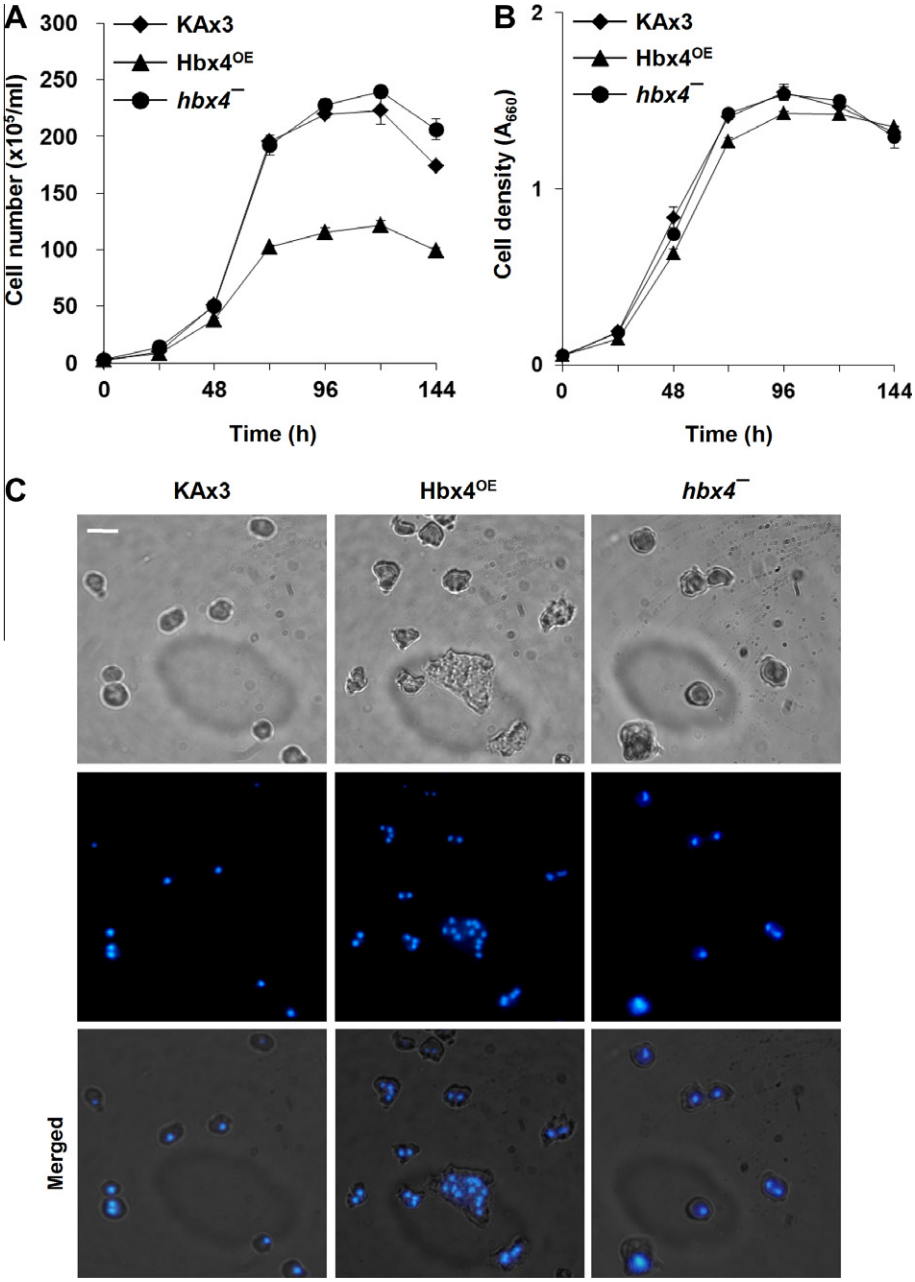

Fig. 3. Hbx4^{OE} exhibits defects in growth rate and cytokinesis in shaken suspension cultures. The cells were grown in suspension culture. (A and B) Their growth was characterized by the increase in density of the cell (A) and turbidity (B). The values represent the mean ± S.E.M. of three independent experiments. (C) Log-phase cells that were grown in suspension were fixed and stained with DAPI. The phase-contrast images (upper panels), DAPI images (middle panels), and merged images (lower panels) are shown. Scale bar: 40 μm.

with 3 μg/ml of TRITC-conjugated phalloidin (Sigma) for 1 h and washed three times with PBS. Cells were stained with 0.1 μg/ml of DAPI (Sigma) and observed under a fluorescent microscope.

2.7. Assay of cell cohesion and growth rate

Cell cohesion assays were performed as previously described [14]. To determine the growth rate, cells of 2×10^5 cells/ml were inoculated in fresh HL5 medium. Their growth was monitored for 144 h and characterized by an increase in cell number and turbidity in suspension culture (absorbance at 660 nm).

2.8. Electrophoretic mobility shift assay (EMSA)

EMSA experiments were performed with purified Hbx4 and FAM-labeled probe as previously described [15,16]. The region encoding the homeodomain was introduced into a pET15b vector and induced using 1 mM IPTG in *Escherichia coli* BL21 (DE3). The Hbx4 protein was purified using Ni^+-column and immediately desalted by dialysis. To generate probes, we divided the 1 kb of gDNA that was upstream of the *cadA* ORF into six overlapping fragments (probe A–F) of 349, 473, 450, 390, 488 and 354 bp using the primers described in Table 1. To identify the Hbx4-binding site, probes that bound to Hbx4 (probe A and C) were divided into about

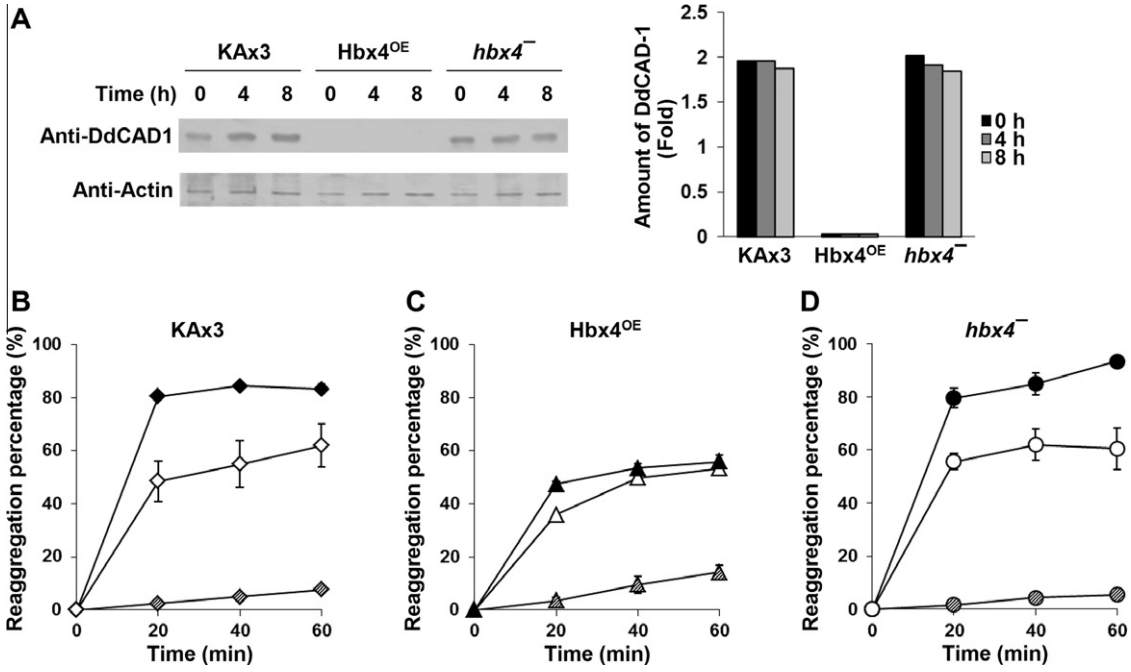

Fig. 4. Hbx4 regulates the expression level of DdCAD-1. (A) Western blot analysis was performed using total protein of developed cells. Membranes were probed with anti-DdCAD-1 and anti-Actin antisera (left). The fold increase of bands corresponding to DdCAD-1 over Actin is shown (right). (B–D) DdCAD-1-dependent cohesion assay is shown. KAx3 (B), Hbx4^{OE} (C) and *hbx4*$^{-}$ (D) cells were developed in KK2 buffer for 4 h. Cells were then dissociated by vortexing, and cell reassociation was assayed in the presence of 10 mM EDTA (cross-hatched symbols) or 10 mM EGTA (open symbols), or in their absence (filled symbols). The values represent the mean ± S.E.M. of three independent experiments.

100-bp fragments (probe G–I) and used for EMSA. The 31-bp oligonucleotide was finally used, which is shown in Fig. 4D (upper strand: 5′-GATGGTTATGATGAATTAATATCAGAATTAT-3′; upper strand of core region mutant: 5′-GATGGTTATGATGAACGCATATCA GAATTAT-3′; the underlined region indicates mutated sequences).

3. Results

3.1. Hbx4^{OE} exhibits the defects in developmental morphology and slug motility

During development, the mRNA level of *hbx4* was increased gradually after 8 h and reached a peak in 24 h (Fig. 1B). To study the function of Hbx4 in vivo, we generated mutant strains that overexpressed Hbx4 (Hbx4^{OE}) or expressed disrupted Hbx4 (*hbx4*$^{-}$). During development, Hbx4^{OE} formed large loose aggregates, which were separated into small aggregates (Fig. 1C). Unlike KAx3, Hbx4^{OE} also produced a fruiting body, which has a short stalk and large glassy sorus (Fig. 1C and D). *hbx4*$^{-}$ exhibited an initial delay development but proceeded to complete the developmental cycle. Whereas KAx3 and *hbx4*$^{-}$ formed migrating slugs in dark conditions, Hbx4^{OE} produced stubby slugs that were unable to migrate (Fig. 1E). The chemotaxis assay [17], which tested the response to cAMP, showed no differences between KAx3 and Hbx4^{OE}. These results suggest that the defect of Hbx4^{OE} in early development was not caused by defects in chemotaxis or cAMP signaling (Supplementary Fig. 1).

3.2. Hbx4 regulates cell-type proportioning

To examine the spatial pattern of cell types, Hbx4^{OE} was marked with *ecmAO*/*lacZ* [18] or stained with neutral red. In Hbx4^{OE} slugs, the expression of *ecmAO*/*lacZ* and the areas of neutral red-stained were extended towards the posterior of the slug and covered >50% of the slug, indicating that they had a significantly enlarged prestalk region. In Hbx4^{OE}, a large number of cells remained as a

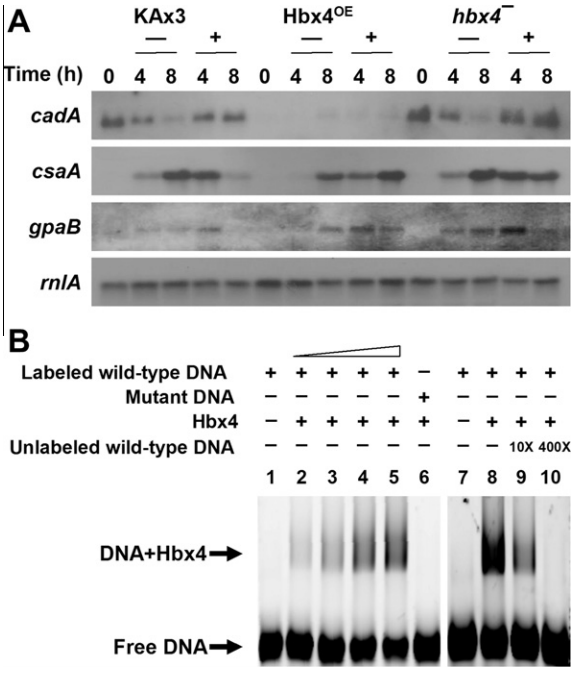

Fig. 5. (A) Hbx4 represses the expression of *cadA*. Axenically grown cells were developed separately in KK2 buffer (pH 6.2) without (−) or with cAMP pulse (+). Total RNA samples were isolated from cells at 0, 4, and 8 h after development and subjected to Northern blot analysis, which used *cadA*, *csaA*, and *gpaB* probes. The *rnlA* probe was used as a loading control. (B) The *cadA* promoter contains the Hbx4-binding site. We identified the Hbx4-binding site in a 1-kb region upstream of the *cadA* ORF as described in the Section 2. An oligonucleotide fragment containing the Hbx4-binding site was used for EMSA. The wild-type oligonucleotide was mixed with buffer (lane 1) or purified Hbx4 protein (lanes 2–5). As the concentration of wild-type oligonucleotide was increased, the binding intensity was also increased (lanes 2–5). Binding was completely abolished by the addition of an oligonucleotide that contained the core motif 'TAAT', which was mutated (lane 6). The binding specificity was determined by the competition assay using 40- or 100-fold excess of unlabeled probes (lanes 9, 10).

mass at the base of the fruiting body (Fig. 1D) and the yield of viable spore production is dramatically reduced by 90% (Fig. 2A and B). In contrast, *hbx4*⁻ slug was composed of the increased prespore region and the decreased prestalk region. However, the *hbx4*⁻ slugs produced mature fruiting bodies.

In Hbx4^{OE}, no expression of the prespore/spore-specific genes, which included *cotC*, *pspA* and *spiA*, was detected. However, the expression levels of the prestalk-specific genes *ecmA* and *ecmB* were higher than those in KAx3 (Fig. 2C). This result is consistent with the morphological analysis and the cell-type proportioning study. The cell adhesion molecule *cadA* was barely expressed in Hbx4^{OE}, whereas the other cell adhesion molecules *csaA* and *lagC* were expressed. *hbx4*⁻ also showed delayed expression of developmental genes with the exception of the spore-specific genes *spiA* and *cadA* compared to KAx3. These results imply that Hbx4 regulates cell-type proportioning and the expression of prespore/spore-specific genes.

Cell type-specific genes were induced in response to exogenous cAMP and DIF in cells that were cultured in suspension. As shown in Fig. 2D, KAx3 exhibited a vigorous induction of *cotC* and *ecmA* that mediated by exogenous cAMP. Under these conditions, DIF, which is required for *ecmA* expression, is supplied endogenously by the cells [19]. In the presence of exogenous cAMP, Hbx4^{OE} increased *ecmA* expression compared to KAx3. However, no *cotC* expression was detected in Hbx4^{OE}. These results are consistent with inability of the Hbx4^{OE} to express prespore-specific genes and show that this defect is not caused by deficiencies in cAMP signaling.

3.3. Hbx4^{OE} exhibits a defect in cytokinesis

In suspension culture, Hbx4^{OE} displayed a greater increase in cell size and a lower growth rate compared to KAx3 and *hbx4*⁻ (Fig. 3A). In contrast, the increase in turbidity, which was used as an indicator of increased cell mass, was similar among the three strains (Fig. 3B). To address the possibility that this phenomenon is caused by a cytokinesis defect, log phase-growing cells were stained using DAPI as described in Section 2. In suspension, Hbx4^{OE} produced large multinucleate cells, whereas most of *hbx4*⁻ and KAx3 were mononuclear or dinuclear cells (Fig. 3C). These results demonstrate that Hbx4^{OE} exhibits defects in cytokinesis.

3.4. Hbx4 regulates the expression of the cell adhesion molecule DdCAD-1

Hbx4^{OE} and *cadA*⁻ showed very similar defects in cell-type proportioning and developmental morphology [14]. Hbx4^{OE} did not express detectable levels of DdCAD-1 (Figs. 2C and 4A). The reassociation of Hbx4^{OE} was significantly diminished by 46% compared to that of KAx3 despite absence of EDTA (Fig. 4B and C). In contrast, the *hbx4*⁻ reassociation was similar to that of KAx3 (Fig. 4D). Because gp80 encoded by *csaA* was not yet expressed at this time, only EDTA/EGTA-sensitive cell adhesion by DdCAD-1 was present. In the presence of EDTA, the adhesion abilities were completely inhibited. The EGTA inhibited the reassociation of KAx3 by 50% but exerted no effect on Hbx4^{OE}. We observed that *cadA* expression was not induced in Hbx4^{OE} by extracellular cAMP although *csaA* and *gpaB* were stimulated (Fig. 5A). A mutant lacking functional Gα2, which was encoded by *gpaB*, failed to enhance *cadA* expression [20]. Extracellular cAMP induced the expression of *cadA* in KAx3 and *hbx4*⁻ (Fig. 5A). These results show that Hbx4 represses the expression of DdCAD-1 and interrupts the induction of *cadA* by extracellular cAMP.

3.5. Hbx4 binds to the cadA promoter

To examine the possibility that Hbx4 acts as a transcriptional regulator of *cadA*, EMSA was performed (Fig. 5B). The *cadA* promoter region containing Hbx4-binding site was determined by EMSA using various pieces of the *cadA* promoter (Table 1) as described in Section 2. Hbx4 did not bind to the probe that contained a core motif 'TAAT' that was mutated in a 31-bp oligonucleotide region containing the Hbx4-binding site. The binding specificity was also determined using the competition assay with an excess amount of unlabeled probes. EMSA results show that *cadA* promoter contains the Hbx4-binding site(s) and that Hbx4 can regulate the *cadA* expression.

3.6. DdCAD-1 overexpression rescues the defects in cytokinesis and development

To corroborate the relationship between Hbx4 and DdCAD-1, DdCAD-1 was constitutively expressed as described in Section 2 (Fig. 6A and B). The aberrant morphology and reduced migration

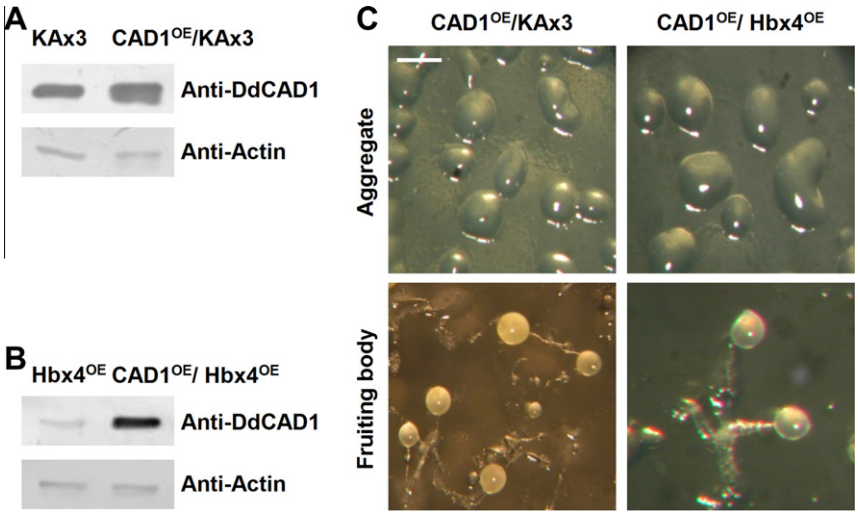

Fig. 6. DdCAD-1 overexpression partially rescues the developmental defects in Hbx4^{OE}. CAD1^{OE}/KAx3 (A) and CAD1^{OE}/Hbx4^{OE} (B) were confirmed by Western blot analysis, which probed with anti-DdCAD-1 and anti-Actin antisera. (C) CAD1^{OE}/Hbx4^{OE} produced normal aggregates (upper). They made fruiting bodies, which had spores with reduced viability, compared to KAx3 (lower). Scale bar: 0.5 mm.

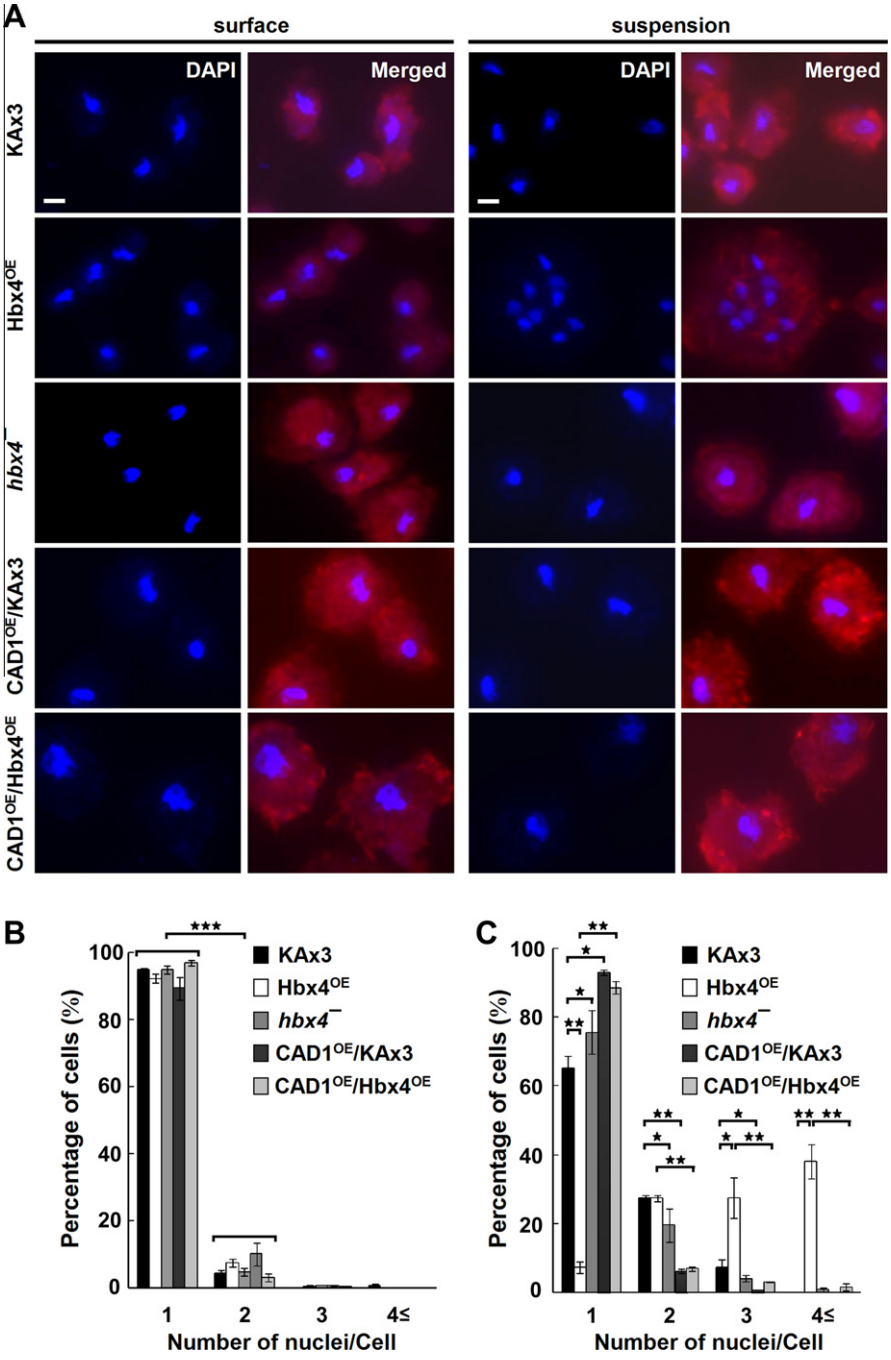

Fig. 7. DdCAD-1 overexpression rescues the cytokinesis defect in Hbx4^{OE}. (A) Double fluorescence staining was performed using TRITC-conjugated phalloidin to label actin filaments and DAPI to label nuclei in cells, which were grown on glass surfaces or in suspension. The first columns of the substrate and suspension panels show DAPI staining. The middle columns of the substrate and suspension panels show the staining for actin filaments. The last columns of the substrate and suspension panels are merged images. Scale bar: 5 μm. (B and C) Histograms show the distribution of nuclei/cell of cells that were grown on glass surface or in suspension. (B) Cells cultured in suspension were grown for 3 more days after being transferred to a glass coverslip and stained with DAPI. n = 163 (KAx3), n = 192 (Hbx4^{OE}), n = 174 (*hbx4*$^{-}$), n = 170 (CAD1^{OE}/KAx3), n = 178 (CAD1^{OE}/Hbx4^{OE}). The values represent the mean ± S.E.M. of three independent experiments. $^{***}P < 0.0005$. (C) Cells cultured in suspension were stained with DAPI, and the counting of nuclei was performed immediately. n = 66 (KAx3), n = 72 (Hbx4^{OE}), n = 71 (*hbx4*$^{-}$), n = 64 (CAD1^{OE}/KAx3), n = 84 (CAD1^{OE}/Hbx4^{OE}). The values represent mean ± S.E.M. of three independent experiments. $^{*}P < 0.05$; $^{**}P < 0.005$.

of Hbx4^{OE} were rescued in CAD1^{OE}/Hbx4^{OE} (Fig. 6C). The spore yield defect was also slightly recovered but maintained at a lower rate compared to the spore yield of KAx3 (data not shown).

To observe the effect of DdCAD-1 overexpression on cytokinesis, we performed double-fluorescence staining in cells, which were cultured in suspension and on a solid substrate, using DAPI for DNA and TRITC-phalloidin for F-actin. In suspension, the distribution of F-actin was polarized in the cortex of KAx3 and *hbx4*$^{-}$ and depolarized in multinucleate Hbx4^{OE} (Fig. 7A). Interestingly, Hbx4^{OE} exhibited different distributions in the types of nuclei in cells that were attached to solid substrate. On solid substrates, 92.22% of Hbx4^{OE} were mononucleated (Fig. 7B), whereas only 7.14% of Hbx4^{OE} were mononucleated in suspension (Fig. 7C). These results suggest that Hbx4^{OE} displays more defects in suspension culture. Unexpectedly, the cytokinesis defect of Hbx4^{OE} was dramatically recovered in CAD1^{OE}/Hbx4^{OE} (Fig. 7A–C). This result indicates that Hbx4 and DdCAD-1 are involved in cell cycle-coupled cytokinesis in suspension [21]. These results are very

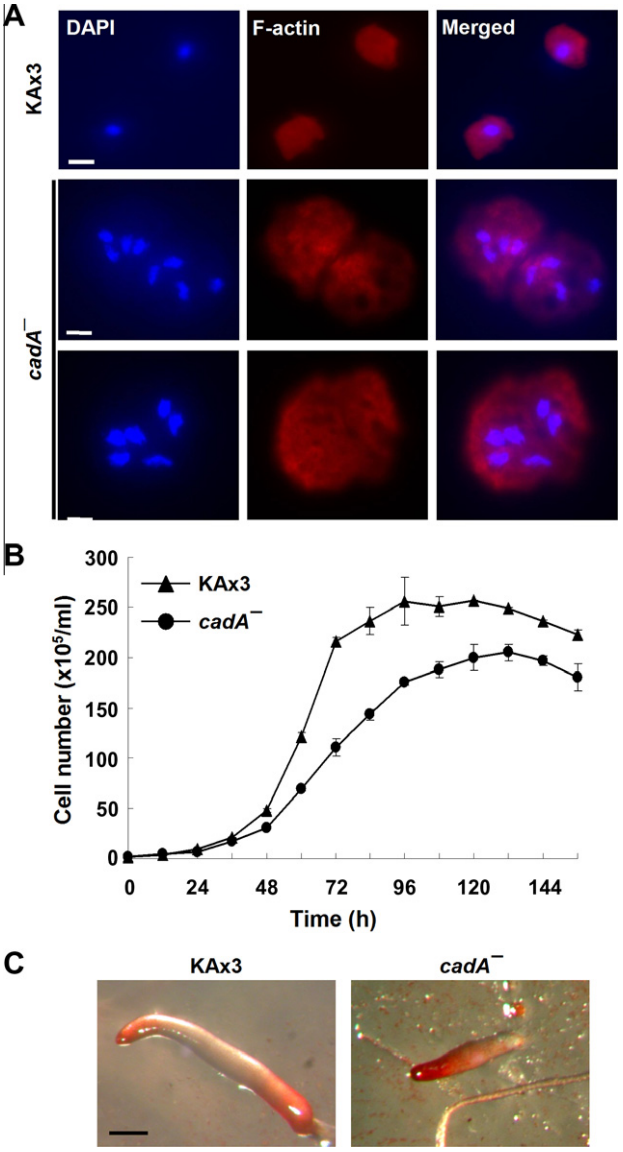

Fig. 8. *cadA*⁻ cells show defects in cell-type proportioning and cytokinesis. (A) Log-phase cells that were grown in suspension were fixed using 1% formaldehyde in methanol. Cells were stained with TRITC-conjugated phalloidin to label actin filaments and with DAPI to label nuclei. The upper panels are KAx3 and the lower panels are *cadA*⁻. The first column of panels shows DAPI staining to identify the nuclei. The middle column of panels shows TRITC-conjugated phalloidin to identify the actin filaments. Merged images of the different channels are shown in the last column. Scale bar: 5 μm. (B) The growth rate of *cadA*⁻ was measured during 156 h in a shaken suspension. The values represent the mean ± S.D. of two independent experiments. (C) The analysis of aberrant cell-type proportioning in *cadA*⁻ cells was performed by staining with neutral red dye. Scale bar: 0.4 mm.

interesting because the function of DdCAD-1 has only been investigated with respect to its role in cell adhesion. We observed that *cadA*⁻ showed defects in growth rate and cytokinesis (Fig. 8A and B). Like Hbx4^{OE}, *cadA*⁻ exhibited defects in cell-type proportioning (Fig. 8C) as previously reported [14]. Our results suggest that Hbx4 acts as a transcriptional regulator of DdCAD-1, which is involved in cytokinesis and development in *D. discoideum*.

4. Discussion

In the current study, we have demonstrated that Hbx4 plays important roles in cytokinesis and development by modulating DdCAD-1. This implies that DdCAD-1 is involved in cytokinesis in addition to cell–cell adhesion. DdCAD-1 shows significant similarities to cadherin with the exception that DdCAD-1 lacks a transmembrane domain [7]. Unlike canonical cadherins, T-cadherin, which also lacks a transmembrane domain, is involved in cytokinesis or centrosomal replication. T-cadherin also acts as a signaling receptor that participates in the recognition of the environment and in the regulation of cell motility and proliferation [22,23]. Whereas most cell adhesion molecules are localized in cell–cell contacts, DdCAD-1 is located in the cytosol and is redistributed in cell membrane by the vacuole as the development is initiated [24]. Therefore, we propose that DdCAD-1 may participate in signaling pathway that controls the growth.

The overexpression of Hbx4 caused obvious defects, whereas its disruption did not show any significant differences compared to that of KAx3 with the exception of cell-type proportioning. Surprisingly, *hbx4*⁻ did not express higher or steady *cadA* mRNA. This result may be due to functional redundancy and interaction/competition between the homeoproteins. There are many reports that demonstrate that the alteration of Hox genes yields ambiguous phenomena because of their complicated action [2,25–27]. Aside from the evidence that there is functional redundancy between paralogous genes, the evidence for functional redundancy between neighboring genes and non-paralogous genes in separate clusters has also been found in mammals [25,26]. We hypothesize that functional redundancy exists in 15 Hox genes of *D. discoideum* *wri* (*hbx1*) and *hbx2*. *hbx2*⁻ has no overt phenotype. However, *wri*(*hbx1*)⁻/*hbx2*⁻ has defects in cell-type proportioning [5]. *wri*⁻/*hbx2*⁻ have slightly stronger defects compared to *wri*⁻. This result suggests *wri* and *hbx2* may be functionally redundant, which does not necessarily mean that they are functionally equivalent.

Although Hbx4^{OE} and *cadA*⁻ showed very similar defects in cell-type proportioning and developmental morphology, Hbx4^{OE} exhibited more severe defects in viable spore production and fruiting body morphology compared to *cadA*⁻. These results suggest that another gene/protein in addition to *cadA* was affected in Hbx4^{OE}. Homeoproteins often regulate different targets depending on cell conditions by interacting with other ones [28]. Because of the complicated characteristics of homeoproteins, many researchers have struggled to identify the Hox's target(s) and to elucidate its mechanism. Hbx4 may modulate another target in addition to *cadA*. We observed that Hbx4 was involved in the expression of the Rho GTPase-related gene (data not shown). And it is possible that Hbx4 may modulate the expression levels of prespore or prestalk specific genes in addition to *cadA*. Consequently, Hbx4^{OE} displayed more severe defects in cell-type proportioning, such as decreased prespore region and increased prestalk region, compared to KAx3 and *cadA*⁻.

Further investigation is required to identify novel Hox genes, which are functionally redundant to Hbx4, and to understand the relationship between DdCAD-1 and target genes of Hbx4.

How are bacteria-feeding cells, which do not express DdCAD-1, more likely to form mononucleates than axenic cells? The *phg A* or *phg B* mutant cells that display cytokinesis defects during axenic growth are able to complete cytokinesis when they are grown on bacteria and are able to adhere to a substrate [21,29]. Similar to the mutants described above, Hbx4^{OE} also did not express DdCAD-1 and exhibited cytokinesis defects in suspension culture, but not on substrate culture (Fig. 7). Myosin expression was normal in Hbx4^{OE} (data not shown). Therefore, we suppose that bacterially growing cells may divide with cell-substrate adhesion despite the absence of *cadA*.

The results shown in the current study will provide novel insights into the relationships between homeoproteins and cell–cell adhesion molecules, between homeoproteins and cytokinesis, and between cell–cell adhesion molecules and cytokinesis in *D. discoideum*. Detailed analyses investigating the mechanisms of

Hbx4-mediated DdCAD-1 expression and DdCAD-1-mediated signal pathways may improve our understanding of the growth and development in metazoans as well as in *D. discoideum*.

Acknowledgments

We thank Dr. R.A. Firtel for providing the EXP4(+) and pA15Gal vectors, Dr. J.G. Williams for providing the pspAGal expression vectors, Dr. C.H. Siu for providing the anti-DdCAD-1 antiserum, and Dr. Chang-Hun Lee for providing preliminary data. *cadA*$^{-}$cells were obtained from the Dicty Stock Center. This work was supported by the Korea Research Foundation Grant, which is funded by the Korean Government (MOEHRD, Basic Research Promotion Fund) (KRF-2007-341-C00261). This work was also supported by the Research Fellowship of the BK21 project.

Appendix A. Supplementary data

Supplementary data associated with this article can be found, in the online version, at doi:10.1016/j.febslet.2011.04.052.

References

[1] Hu, G., Lee, H., Price, S.M., Shen, M.M. and Abate-Shen, C. (2001) Msx homeobox genes inhibit differentiation through upregulation of *cyclin D1*. Development 128, 2373–2384.
[2] Ford, H.L. (1998) Homeobox genes: a link between development, cell cycle, and cancer? Cell Biol. Int. 22, 397–400.
[3] Greenstein, D., Hird, S., Plasterk, R.H., Andachi, Y., Kohara, Y., Wang, B., Finney, M. and Ruvkun, G. (1994) Targeted mutations in the *Caenorhabditis elegans* POU homeo box gene *ceh-18* cause defects in oocyte cell cycle arrest, gonad migration, and epidermal differentiation. Genes Dev. 8, 1935–1948.
[4] Argiropoulos, B. and Humphries, R.K. (2007) Hox genes in hematopoiesis and leukemogenesis. Oncogene 26, 6766–6776.
[5] Han, Z. and Firtel, R.A. (1998) The homeobox-containing gene *Wariai* regulates anterior-posterior patterning and cell-type homeostasis in *Dictyostelium*. Development 125, 313–325.
[6] Sillo, A., Bloomfield, G., Balest, A., Balbo, A., Pergolizzi, B., Peracino, B., Skelton, J., Ivens, A. and Bozzaro, S. (2008) Genome-wide transcriptional changes induced by phagocytosis or growth on bacteria in *Dictyostelium*. BMC Genomics 9, 291.
[7] Wong, E.F., Brar, S.K., Sesaki, H., Yang, C. and Siu, C.H. (1996) Molecular cloning and characterization of DdCAD-1, a Ca^{2+}-dependent cell–cell adhesion molecule, in *Dictyostelium discoideum*. J. Biol. Chem. 271, 16399–16408.
[8] Jeong, S.Y., Choi, C.H., Kim, J.S., Park, S.J. and Kang, S.O. (2006) Thioredoxin reductase is required for growth and regulates entry into culmination of *Dictyostelium discoideum*. Mol. Microbiol. 61, 1443–1456.
[9] Galardi-Castilla, M., Pergolizzi, B., Bloomfield, G., Skelton, J., Ivens, A., Kay, R.R., Bozzaro and Sastre, L. (2008) SrfB, a member of the Serum Response Factor family of transcription factors, regulates starvation response and early development in *Dictyostelium*. Dev. Biol. 316, 260–274.
[10] Weijer, C.J., David, C.N. and Sternfeld, J. (1987) Vital staining methods used in the analysis of cell sorting in *Dictyostelium discoideum*. Methods Cell Biol. 28, 449–459.
[11] Haberstroh, L. and Firtel, R.A. (1990) A spatial gradient of expression of a cAMP-regulated prespore cell-type-specific gene in *Dictyostelium*. Genes Dev. 4, 596–612.
[12] Dynes, J.L., Clark, A.M., Shaulsky, G., Kuspa, A., Loomis, W.F. and Firtel, R.A. (1994) LagC is required for cell–cell interactions that are essential for cell-type differentiation in *Dictyostelium*. Genes Dev. 8, 948–958.
[13] Imai, K., Kijima, T., Noda, Y., Sutoh, K., Yoda, K. and Adachi, H. (2002) A Rho GDP-dissociation inhibitor is involved in cytokinesis of *Dictyostelium*. Biochem. Biophys. Res. Commun. 296, 305–312.
[14] Wong, E., Yang, C., Wang, J., Fuller, D., Loomis, W.F. and Siu, C.H. (2002) Disruption of the gene encoding the cell adhesion molecule DdCAD-1 leads to aberrant cell sorting and cell-type proportioning during *Dictyostelium* development. Development 129, 3839–3850.
[15] Coqueret, O., Berube, G. and Nepveu, A. (1998) The mammalian Cut homeodomain protein functions as a cell-cycle-dependent transcriptional repressor which downmodulates $p21^{WAF1/CIP1/SDI1}$ in S phase. EMBO J. 17, 4680–4694.
[16] Scott, V., Clark, A.R. and Docherty, K. (1994) The gel retardation assay. Methods Mol. Biol. 31, 339–347.
[17] Root, P.A., Prince, A. and Gundersen, R.E. (1999) Aggregation of *Dictyostelium discoideum* is dependent on myristoylation and membrane localization of the G protein alpha-subunit, G alpha 2. J. Cell Biochem. 74, 301–311.
[18] Early, A.E., Gaskell, M.J., Traynor, D. and Williams, J.G. (1993) Two distinct populations of prestalk cells within the tip of the migratory *Dictyostelium* slug with differing fates at culmination. Development 118, 353–362.
[19] Yasukawa, H., Mohanty, S. and Firtel, R.A. (1998) Identification and analysis of a gene that is essential for morphogenesis and prespore cell differentiation in *Dictyostelium*. Development 125, 2565–2576.
[20] Yang, C., Brar, S.K., Desbarats, L. and Siu, C.H. (1997) Synthesis of the Ca(2+)-dependent cell adhesion molecule DdCAD-1 is regulated by multiple factors during *Dictyostelium development*. Differentiation 61, 275–284.
[21] Nagasaki, A., de Hostos, E.L. and Uyeda, T.Q. (2002) Genetic and morphological evidence for two parallel pathways of cell-cycle-coupled cytokinesis in *Dictyostelium*. J. Cell Sci. 115, 2241–2251.
[22] Andreeva, A.V., Kutuzov, M.A., Tkachuk, V.A. and Voyno-Yasenetskaya, T.A. (2009) T-cadherin is located in the nucleus and centrosomes in endothelial cells. Am. J. Physiol. Cell Physiol. 297, C1168–C1177.
[23] Philippova, M., Joshi, M.B., Kyriakakis, E., Pfaff, D., Erne, P. and Resink, T.J. (2009) A guide and guard: the many faces of T-cadherin. Cell. Signal. 21, 1035–1044.
[24] Sriskanthadevan, S., Lee, T., Lin, Z., Yang, D. and Siu, C.H. (2009) The cell adhesion Molecule DdCAD-1 is imported into contractile vacuoles by membrane invagination in a Ca^{2+}- and conformation-dependent manner. J. Biol. Chem. 284, 36377–36386.
[25] Savory, J.G., Pilon, N., Grainger, S., Sylvestre, J.R., Béland, M., Houle, M., Oh, K. and Lohnes, D. (2009) Cdx1 and Cdx2 are functionally equivalent in vertebral patterning. Dev. Biol. 330, 114–122.
[26] van den Akker, E., Fromental-Ramain, C., de Graaff, W., Le Mouellic, H., Brûlet, P., Chambon, P. and Deschamps, J. (2001) Axial skeletal patterning in mice lacking all paralogous group 8 Hox genes. Development 128, 1911–1921.
[27] Pramila, T., Miles, S., GuhaThakurta, D., Jemiolo, D. and Breeden, L.L. (2002) Conserved homeodomain proteins interact with MADS box protein Mcm1 to restrict ECB-dependent transcription to the M/G1 phase of the cell cycle. Genes Dev. 16, 3034–3045.
[28] Hueber, S.D., Bezdan, D., Henz, S.R., Blank, M., Wu, H. and Lohmann, I. (2007) Comparative analysis of Hox downstream genes in *Drosophila*. Development 134, 381–392.
[29] Waddell, D.R., Duffy, K. and Vogel, G. (1987) Cytokinesis is defective in *Dictyostelium* mutants with altered phagocytic recognition, adhesion, and vegetative cell cohesion properties. J. Cell Biol. 105, 2293–2300.